

Optical Engineering

OpticalEngineering.SPIEDigitalLibrary.org

Infrared neurostimulation of earthworm: from modeling to experiment

Mohammad Ali Ansari
Valery V. Tuchin

SPIE.

Mohammad Ali Ansari, Valery V. Tuchin, "Infrared neurostimulation of earthworm: from modeling to experiment," *Opt. Eng.* **59**(6), 061627 (2020), doi: 10.1117/1.OE.59.6.061627

Infrared neurostimulation of earthworm: from modeling to experiment

Mohammad Ali Ansari^{a,*} and Valery V. Tuchin^{b,c,d}

^aShahid Beheshti University, Laser and Plasma Research Institute, Tehran, Iran

^bSaratov State University, Research-Educational Institute of Optics and Biophotonics,
Saratov, Russia

^cTomsk State University, Interdisciplinary Laboratory of Biophotonics, Tomsk, Russia

^dRussian Academy of Sciences, Institute of Precision Mechanics and Control,
Laboratory of Laser Diagnostics of Technical and Living Systems, Saratov, Russia

Abstract. Infrared neurostimulation (INS) is a new approach for modulation or control of neuronal pulses. Recently, different studies have been presented to investigate the origin of generation of the action potentials during INS, and it seems that the photothermal mechanism has an important role during INS. So, spatial and temporal temperature changes are important parameters, because the heating of neural tissue can excite or block the activity of neurons and an excess deposit of thermal energy could damage the neural tissues. We aim to explore the effects of heat diffusion during INS. We model the generation of action potential using the photothermal mechanism to study the changes of electrical properties of the membrane of neural cell in the earthworm (as a simple neuronal network) during INS. The variation of electrical properties of the membrane causes the changes in the concentration of ions such as K^+ and Na^+ inside the cells, which can originate the action potentials. This study includes three sections: (1) exploring the effect of laser light properties (wavelength of 1450 and 1550 nm, repetition rate and energy per pulse) on the measurement of temperature rise inside a phantom similar to neuronal tissue, (2) theoretical modeling to predict the generation of action potentials induced by the local temperature rise inside the neuronal network of earthworm, and (3) detecting the variation of voltage of peripheral nervous system of the earthworm during INS. This modeling can help us to better understanding the mechanism of the blocking and controlling the action potentials for *in-vivo* applications in the brain cognitive studies and treatment of some neuron system diseases. © 2020 Society of Photo-Optical Instrumentation Engineers (SPIE) [DOI: 10.1117/1.OE.59.6.061627]

Keywords: infrared laser; neuron; stimulation; photothermal.

Paper 191684SS received Dec. 7, 2019; accepted for publication Feb. 18, 2020; published online Mar. 5, 2020.

1 Introduction

The stimulation or inhibitory neuronal activities have important roles in the detection or treatment of certain neuron system diseases.¹⁻³ Recently, infrared (IR) light sources have been applied to modulate the neuronal activities of the heart, cortex, and peripheral nervous system (PNS) in *in-vitro* and *in-vivo* studies.³⁻⁶

In 2005, Wells et al. utilized laser (Holmium:YAG @ 2.12 μm , radiant exposure of 0.3 to 1.2 J/cm^2 at repetition rate of 2 Hz) to stimulate the sciatic nerve in rat. They demonstrated a new artifact-free modality for stimulation of neuron using pulsed IR laser. Also, they noted that the spatial selectivity of infrared neurostimulation (INS), compared to electrical stimulation, provides a good opportunity for mapping and repairing PNS.⁷ In 2010, Jenkins et al., for the first time, applied pulsed laser light (wavelength of 1875 nm, pulse duration of 2 ms, and the radiant exposure of 0.84 mJ/cm^2 per pulse) to demonstrate an optical pacing of a 2-day embryonic quail heart.² They also modulated the heartbeat of rabbit (*in vitro*).⁸ We have recently demonstrated the control of the heartbeat of a rat *in vivo*.⁹ In 2018, Xia and Nyberg studied *in vitro* the effect of

*Address all correspondence to Mohammad Ali Ansari, E-mail: m_ansari@sbu.ac.ir

continuous-wave near-infrared (NIR) laser (wavelength of 1550 nm, laser power 2 to 111 mW, and dose of 30 s) on neuronal activities of embryonic day 18 (E18) Sprague Dawley rat cortex.³

INS provides three advantages: (1) the contact-free delivery system, (2) high spatial precision, and (3) lack of stimulation artifacts. The experimental results show that INS can provide fine spatial resolution, smaller than 0.4 mm, improving the selectivity of neural stimulations.^{9,10} The spatial resolution of INS is a function of the core size of delivery optical fiber, optical properties of biological tissue, the distribution of laser energy deposited, and consequently the local temperature rise inside the tissue.^{10–12}

Although the whole mechanism of INS is not yet completely understood,³ but based on the results shown in the previous studies,^{7,10–15} it seems that the mechanism of INS in the PNS can be explained by photothermal mechanism.¹⁶ Recent experimental and simulation studies show that temperature rise can change membrane capacitance or the membrane ion permeability.^{15,17,18} For example, INS can modulate cortical calcium dynamics or form short-live nanopores, which change the capacitance of membrane. In 2017, Eom et al.¹⁷ studied the effects of gold nanorod on activation of astrocyte cultures prepared from cerebral cortices of Sprague Dawley rat. They indicated that local heat induces asymmetrical displacement of ions within the double layer on both sides of the membrane leading to net charge displacement across the membrane (as an activation of voltage-gated Ca^{2+} channels).

Regardless of the origin of membrane changes (includes modulation calcium gate, formation of nanopores, and variation of capacitance of membrane), the spatial and temporal variations in temperature are the key parameters for INS. Thus, IR laser can excite or block the activity of the neurons. In addition, extra deposited energy can potentially damage the neural targets.^{15,18,19} A fast local temperature rise by the laser energy deposited can change the membrane capacitance,¹⁴ which can generate the action potential.^{9,20–22} In 2018, Plaksin et al.¹⁹ presented a theoretical model, based on solution of electrostatic Boltzmann equation in a flat three-layer membrane, to show that an intramembrane thermal–mechanical effect, wherein the membrane undergoes axial narrowing and lateral expansion, predicts a thermal capacitance increase rate of $\sim 0.3\%/^{\circ}\text{C}$. In 2018, Ebtehaj et al.²¹ developed the previous theoretical model¹⁹ to calculate the membrane electrical capacitance. They modeled lipid bilayer membrane via a flat five-layer structure with infinite lateral extension and finite thickness. They calculated a value of $0.37\%/^{\circ}\text{C}$ for the thermally induced electrical capacitance increase rate.

The previous studies show the importance of heat distribution during INS. In 2013, Liljemalm et al.¹² applied COMSOL Multiphysics® Software to simulate the spatial and temporal temperature distributions for INS of cortical cells *in vitro* (wavelength of 1550 nm and radiant exposure of $5.2 \text{ J}/\text{cm}^2$). We have analytically estimated the distribution of deposited thermal energy inside aqua phantom, similar to human cortical tissue, induced by a train of the IR laser pulses.¹¹ Using these simulated temperature rises and based on temperature dependence of membrane reported *in vitro* by Shapiro et al.¹⁵ and Plaksin et al.,¹⁹ one can estimate the alteration in membrane capacitance, which starts the generation of action potentials. Using simple and giant neuronal network, like earthworm, can help us to better understand the mechanism of INS. The cerebral ganglion of the earthworm is connected to a ventral nerve cord that runs the length of the body, allowing earthworms to move and respond to external stimuli.²³ We recently recorded optically the neuromuscular activity of earthworm via phase-sensitive measurement while stimulating it optically using NIR laser (wavelength of 1550 nm; for frequency range of 3, 5.5, and 7 Hz; and duration time of 3, 5, 8, and 17 ms).²²

Here, we study the generation of the action potentials in PNS of earthworm. To do it and based on our results in the previous studies,^{9,10} we combine the heat diffusion equation and Hodgkin–Huxley (HH) axonal model to simulate how an action potential generates inside PNS of an earthworm. First, we experimentally measure the maximum temperature rise of an aqua phantom, similar to the neuron tissue. These obtained results are applied to simulate how the action potentials generate in PNS of the earthworm. Finally, we apply NIR lasers at wavelengths of 1450 and 1550 nm to modulate the neuronal activities of the earthworm. Hence, the novelties of this study are (1) the usage of a combined thermal-neuronal approach to model the generation of the action potential and (b) noncontact *in-vivo* NIR stimulation of earthworm that provides a complete theoretical INS model in an earthworm as a simple neuronal network. These results can be applied to better understand the mechanism of INS in the complicated neuronal network systems.

2 Theoretical Model and Experimental Setup

First, we consciously explain the thermal approach to simulate the generation of the action potentials. Then, the experimental setup to measure the variation of voltage of PNS of earthworm is explained.

2.1 Theoretical Model

We apply heat diffusion equation²⁴ to simulate the heat distribution inside the body of earthworm:

$$\frac{\partial T}{\partial t} = D\nabla^2 T(\mathbf{r}, t) + \frac{1}{\rho C_P} S(\mathbf{r}, t), \quad (1)$$

where T is the temperature, t is the time, and \mathbf{r} is the spatial coordinate to light propagation, respectively. Here D is the heat conductivity, ρ is the tissue density, and C_P is the specific heat capacity. The S indicates the heat source by laser energy deposited. For simple geometry, such as semifinite¹⁰ and cylindrical shape,²⁴ we can analytically solve Eq. (1). Here, we apply Green's function to solve Eq. (1). The results presented in Refs. 10 and 12 show that the penetration depth of lasers with the wavelength less than 2.0 μm is submillimeter. Hence, we can easily find the Green's function for Eq. (1) (for semi-infinite geometry). The Green's function is described as satisfying the point source equation:²⁵

$$\frac{\partial G(r, z, t; r', z', t')}{\partial t} = D\nabla^2 G(r, z, t; r', z', t') + \frac{1}{\rho C_P} \delta(r - r') \delta(z - z') \delta(t - t'). \quad (2)$$

By assuming $\nabla^2 = \partial^2/\partial r^2 + 1/r\partial/\partial r + \partial^2/\partial z^2$ and applying Hankel transform on observation point r in the previous equation, we have:

$$\frac{\partial G_h}{\partial t} - D \left(\frac{\partial^2 G_h}{\partial z^2} - k^2 G_h \right) = \frac{r'}{\rho C_P} J_0(kr') \delta(z - z') \delta(t - t'), \quad (3)$$

where G_h is the Hankel transform of G :

$$G_h \equiv G_h(k, z, t; r', z', t') = \int_0^\infty G(r, z, t; r', z', t') J_0(kr) r dr. \quad (4)$$

Then we apply Fourier transform on z and obtain:

$$\frac{\partial G_{hf}}{\partial t} + D(k_z^2 + k^2) G_{hf} = \frac{r'}{\sqrt{2\pi\rho C_P}} J_0(kr') e^{ik_z z'} \delta(t - t'), \quad (5)$$

where G_{hf} is the Fourier transform of G_h :

$$G_{hf} \equiv G_{hf}(k, k_z, t; r', z', t') = \int_0^\infty G(k, z, t; r', z', t') e^{ik_z z} dz. \quad (6)$$

Lastly, Laplace transform on t results in

$$[D(k_z^2 + k^2) + s] G_{hfl} = \frac{r'}{\sqrt{2\pi\rho C_P}} J_0(kr') e^{ik_z z'} e^{-st'}, \quad (7)$$

where G_{hfl} is the Laplace transform of G_{hf} :

$$G_{hfl} \equiv G_{hfl}(k, k_z, s; r', z', t') = \int_0^\infty G(k, z, t; r', z', t') e^{-st} dt. \quad (8)$$

Therefore, we get

$$G_{hfl} = \frac{r'}{\sqrt{2\pi\rho C_p}} \frac{J_0(kr')e^{ik_z z'} e^{-st'}}{D(k_z^2 + k^2) + s}. \quad (9)$$

To obtain G , we can respectively apply Laplace, Fourier and Hankel transforms on previous relation as follows:

$$G(r, z, t; r', z', t') = \frac{r' H(t-t')}{\sqrt{2\pi\rho C_p} [2D(t-t')]^{\frac{3}{2}}} e^{\left[\frac{(z-z')^2}{4D(t-t')}\right]} e^{\left[-\frac{r^2+r'^2}{4D(t-t')}\right]} I_0\left[\frac{rr'}{4D(t-t')}\right], \quad (10)$$

where $H(t-t')$ is the Heaviside function and I_0 is the modified Bessel function. The distribution of temperature inside the tissue can be estimated as

$$T(r, t) = \int_0^t \int G(r, z, t; r', z', t') S(r', t') dt' dr'. \quad (11)$$

We can numerically solve this integral to estimate the temperature rise inside the tissue. The local temperature rise obtained by Eq. (11) can change the membrane capacitance as explained by Shapiro et al.¹⁵ and Alemzadeh-Ansari et al.⁹ This temperature dependency of membrane capacitance affects the extracellular potentials. We assume that illuminating laser light has a Gaussian profile, $e^{(-r^2/\sigma^2)}/\pi\sigma^2$ and attenuates with distance z , according to $e^{-\mu_a z}$, where μ_a is the absorption coefficient of the sample.^{11,12} Our numerical results based on Eq. (11) and other presented results^{26,27} show that the temperature rise for IR pulses can be assumed as

$$T = \begin{cases} \Delta T \alpha \frac{t}{\tau_1} & t < \tau_{\text{pulse}} \\ \Delta T [\varphi e^{\frac{-t}{\tau_1}} + (1 - \varphi) e^{\frac{-t}{\tau_2}}] & t > \tau_{\text{pulse}} \end{cases}, \quad (12)$$

where τ_1 , τ_2 , α , and φ can be estimated by experimental data and ΔT is the single pulse temperature rise. The capacitive photothermal depolarization evoked by a single IR pulse can be estimated using²⁶

$$\Delta V \approx \left(\frac{\beta}{c_m}\right) \frac{dT}{dt}, \quad (13)$$

where c_m is the cell membrane capacitance and β is a parameter related to membrane area exposed to IR laser. Experimental results depicts that^{8,28}

$$c_m = c_0 + \frac{\kappa}{\delta T}, \quad (14)$$

where c_0 is $\sim 1.18 \mu\text{F}/\text{cm}^2$ and k is $\sim 2.2 \mu\text{F}/\text{cm}^2 \cdot ^\circ\text{C}$, and δT is $\approx 50 - T$. Hence, temperature dependence of cell membrane capacitance can be shown as follows:

$$\frac{dc_m}{dt} = \frac{\kappa}{\delta T^2} \frac{c_m}{\beta} \Delta V. \quad (15)$$

The experimental results show that action potentials depict a threshold and a sudden rise in membrane voltage and current.²⁸ The total current through the membrane can be given as²⁹

$$I = c_m \left(\frac{dV}{dt}\right) + (V - V_r) \left(\frac{dc_m}{dt}\right). \quad (16)$$

By using Eq. (15) and classical HH model,^{28,29} we have

$$I = c_m \left(\frac{dV}{dt}\right) + g_K(V - V_K) + g_{Na}(V - V_{Na}) + g_l(V - V_l), \quad (17)$$

where g_K , g_{Na} , and g_l are potassium, sodium, and leakage conductance per unit area, respectively. Here V_K and V_{Na} are the reversal potential of potassium and sodium channels and V_l is the reversal potential of leakage.

2.2 Experimental Setup

The experimental procedure includes (1) measurement of temperature inside an aqua phantom and (2) *in-vivo* stimulation of earthworm. First, the temperature rise of an aqua phantom by laser deposited (wavelengths of 1450 and 1550 nm) is measured (the details of experimental setup were shown in Ref. 10). These measured data are applied for simulating the generation of action potentials based on modified Hodgkin–Huxley model (MHHM). In this modified model, we consider the thermal variation of the membrane capacitance as stated in Eq. (15). The details of this simulation were presented by Fribance et al.²⁹ and our group.⁹

Ten earthworms (diameter $\sim 500\ \mu\text{m}$) are kept in a soil box with sufficient temperature and humidity and oxygen. All animals participating in this study were cared for according to the ethic committee of Shahid Beheshti University, Iran. This humidity is necessary since the external part of the earthworm body secretes mucus over the cuticle to maintain the worm body moist and ease its movement through soil.²² In this study, we use a pulsed butterfly laser module (wavelengths of 1450 and 1550 nm, IR-1550, Iran) that their energy and pulse duration can be adjusted up to 6 mJ/pulse and 18 ms, respectively. The laser pulse is delivered to worm via a 200- μm multimode optical fiber [numerical aperture (NA) = 0.22]. The neuronal activities are measured using an active electrode module (Byamed, Iran). Earthworm is placed in a foam-rubber cage that (1) allows one to record electrophysiological signals and (2) prevents awake worms from crawling away. Some pins were pushed through the rubber to record neural signal. Finally, a transparent ruler covers the worm (see Fig. 1).

3 Results and Discussion

This study aims to present an algorithm from laser illumination to generate an action potential based on photothermal mechanism. This process starts by heating the neural tissues, which results in the variation of electrical properties of the neural cell membranes. So, we first simulate the heating of biological phantom and study the effect of laser light properties on maximum temperature rises. To do it, the temperature rise by laser energy (wavelengths of 1450 and 1550 nm, energy of 6 mJ, and repetition rate between 2 and 10 Hz) deposited inside a semi-infinite tissue is estimated and compared with those data presented in previous studies.^{9,10,12} It shows that the model can predict the temperature rise with maximum relative error of 20%. In 2013, a numerical solution based on finite element method (via COMSOL) was presented to simulate heating during INS,¹² and in 2018 a similar work has been done to simulate the maximum temperature rise in a primary cortex slices from embryonic day 18 (E18) Sprague Dawley rat cortex (wavelength of 1550 nm and the maximum temperature increase at the cell layer is

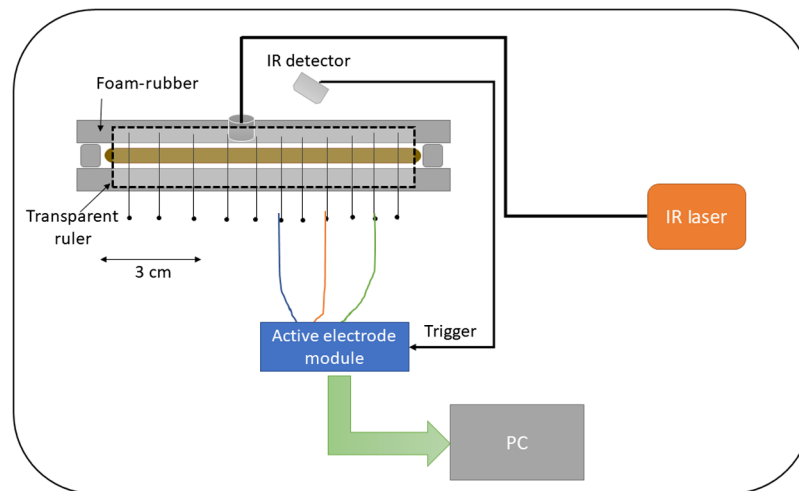


Fig. 1 The cage keeping earthworm. The laser light is delivered to worm via a 200- μm multimode optical fiber. An IR amplified detector (PDA20H, Thorlabs) is used to trigger the active electrode module.

from 0.4°C at a laser power of 2 mW to 16°C at a laser power of 111 mW).³ In the current study, we apply an analytical solution based on the Green’s function, which could easily calculate temperature rises. Schlett et al.,³⁰ in 2019, applied a laser light of 1470 nm (energy of 6 mJ and repetition rate of 0.2 Hz) to stimulate the sciatic nerve of rat. They measured a temperature rise of 6°C that is similar to our results.

The experimental results in Refs. 9 and 30 predict that a temperature rise less than 6°C, induced by a train of IR pulse laser, can be a starting point to achieve INS. Using an analytical method helps us to adjust the laser light parameters to achieve this temperature rise. We apply phantom study to verify this hypothesis. So, the laser pulse is delivered to a distilled water-filled Petri dish via a multimode optical fiber (core size = 200 μm, NA = 0.22), because the absorption coefficient of nerve tissue and water for spectrum 1400 to 1600 nm are similar.^{9,10} Figure 2 depicts the variation of temperature versus the repetition rate of lasers. One can see that an increase in the repetition rate increases the maximum of temperature of phantom. Results presented by Schlett et al.³⁰ show that in contrast to single-pulse stimulation, higher repetition rates lead to cumulative temperature buildup, and data in Fig. 2 confirm this issue.

Figure 3 shows the effect of pulse duration on the temperature. These figures illustrate that a wavelength of 1450 nm causes more heat inside the phantom. This is because the absorption coefficient of neuronal tissue at this wavelength (corresponding to maximum of the strong water

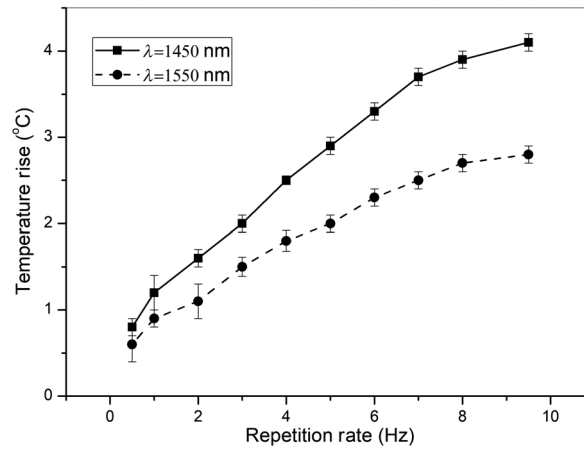


Fig. 2 Variation of temperature for two different wavelengths of 1450 and 1550 nm versus the repetition rate. Pulse duration is 18 ms and energy per pulse for 1450 and 1550 nm are 5 and 6 mJ, respectively.

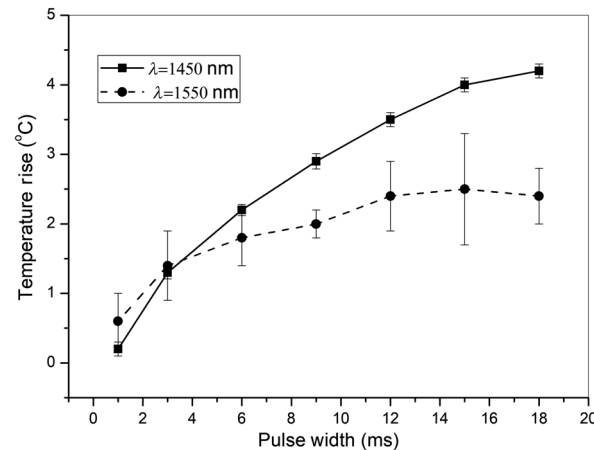


Fig. 3 The effects of pulse duration on the temperature. The repetition rate is 9.5 Hz and energy per pulse for 1450 and 1550 nm are 6 and 8 mJ, respectively.

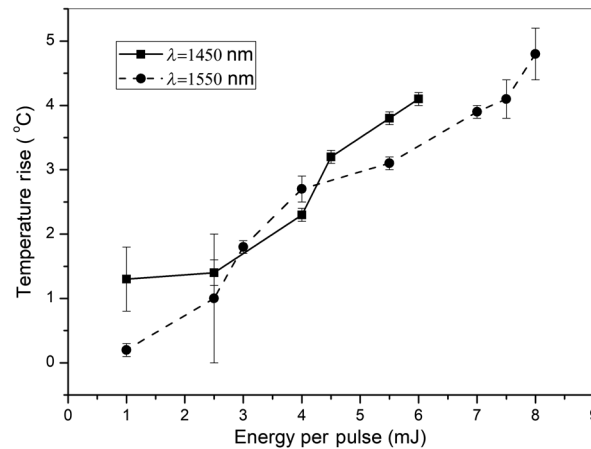


Fig. 4 The variation of temperature induced by different energy per pulse. Pulse duration is 18 ms and repetition rate is 9.5 Hz.

band) is greater than the wavelength of 1550 nm. The impact of energy per pulse on the temperature is shown in Fig. 4.

These results show that, for used laser parameters, the maximum temperatures reach 5.5°C. These measurements are applied to predict the threshold temporal temperature required to initiate an action potential in earthworm. We simulate the generation of action potentials inside axonal model of earthworm using MHHM.^{9,29} The results are obtained during 20 ms after heating the tissue. Figure 5(a) depicts a sudden rise in the membrane voltage by a temperature rise of 5.4°C, as we expected.^{29,7} Our results show that this action potential is propagated inside a typical axon of the earthworm. Figures 5(a) and 5(b) illustrate the membrane capacitance and total current. These results confirm the possibility of generation of action potentials inside PNS of the earthworm using NIR laser (wavelengths of 1550 and 1450 nm). Plaksin et al.¹⁹ predicted a thermal capacitance increase rate of 0.30%/°C and Ebtehaj et al.,²¹ in 2018, theoretically illustrated that the mentioned increase is a function of pulse energy and it can be a value between 0.26%/°C and 0.65%/°C for pulses from 2.8 to 7.3 mJ, respectively. Our results approximately show an increase rate less than 0.5%/°C for pulse energy less than 6 mJ that can be compatible with those predictions by Ebtehaj et al.²¹

Finally, the NIR laser light is applied to stimulate the nerve cord of the worm. We use an IR detector to trigger the recording device. The electrical signal is measured by an accurate electrophysiological system. The laser light (pulse duration of 18 ms and repetition rate of 0.5 Hz) is guided to the worm via a multimode fiber. Figure 6 shows the variation of measured voltage after three laser pulses (wavelength of 1450 nm). One can see that we use a low-level laser energy to stimulate the PNS of the earthworm. To better understand the mechanism of INS, we have to study the impact of laser parameters (laser energy, repetition rate, and pulse duration) on the generation of action potential. The origination of action potentials need a threshold of laser energy, so we change the laser energy from 1 to 6 mJ to find the threshold amount of energy. We found that the energy around the 5 mJ is a good choice to originate action potential that this amount of energy per pulse is predicted via simulation data, as presented in Fig. 5. Moreover, an increase in pulse duration arises the measured voltage. Hence, we utilize pulse duration of 18 ms.

In addition, we apply 1550 nm laser light, but we cannot see a significant INS stimulation. As explained in Ref. 9, the absorption coefficient at lambda of 1450 nm is three times larger than lambda of 1550 nm, and so we require more radiant energy, which burns the worm. Recently, Throckmorton et al.³¹ compared the INS efficiency using two wavelengths, 1450 and 1875 nm. Their results indicate that $\lambda = 1450$ nm needs lower energy to activate threshold activation as compared to $\lambda = 1875$ nm, whereas the 1875-nm light can activate deeper nerve fibers.³¹

Here, we note that the rapid heat changes can initiate an activation process inside the neuron tissue, but we need more studies to completely understand this process and the recent studies suggest that the temperature rise can alter the membrane properties and ion channel kinetics.^{31–34} In previous investigations, we studied the effect of the axon diameter and global axon

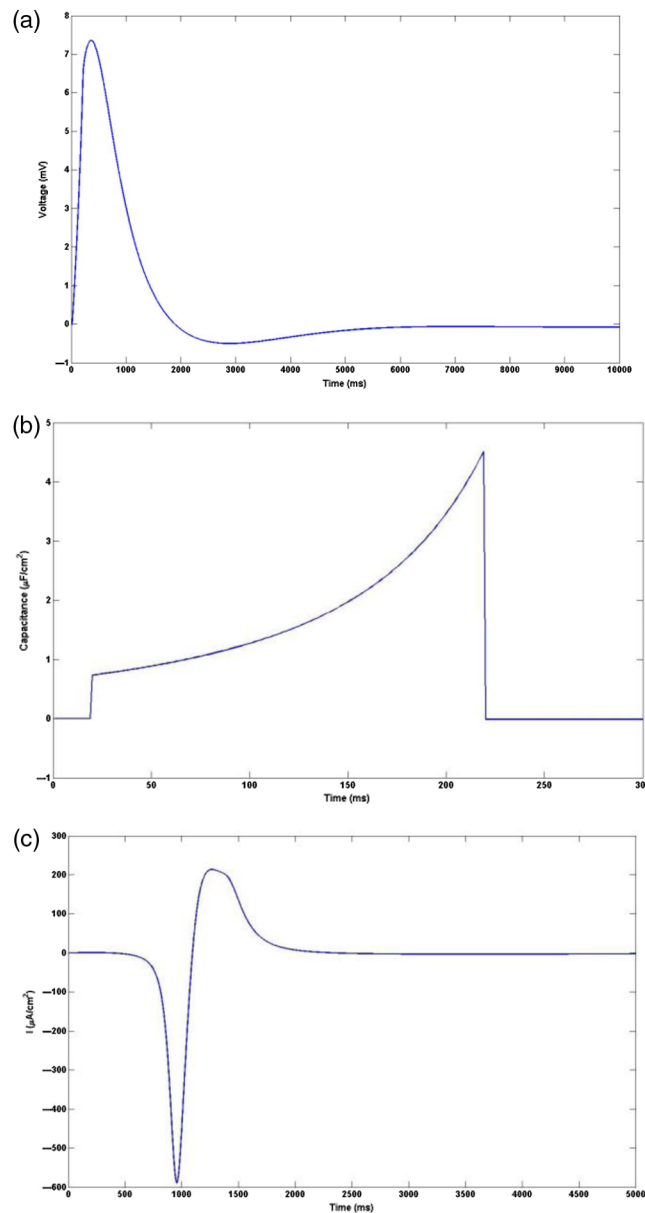


Fig. 5 The generation of action potential. (a) The temporal variation of extracellular voltage during INS inside the neuronal system of earthworm. (b) The temporal variation of membrane capacitance and (c) the variation of current during INS. The constant values applied in this simulation are $g_{Na} = 120$, $g_K = 36$, $g_l = 0.1$ (m.mho/cm²), $V_{Na} = -110$ mV, $V_K = 15$ mV, $V_l = -10.6$ mV.³²

temperature on threshold activation.⁹ Our results show that small-diameter axon can activate at low radiant energy, which are in agreement with those results presented by Lothet et al.,³⁴ Beier et al.³⁵ in 2014 showed that 1870 nm laser light can form some short-live nanopores in the plasma membrane allowing the influx of extracellular ions (via a temperature rise of 20°C). It seems that the formation of nanopores can alter the membrane capacitance. Moen et al. developed a nonlinear imaging based on second harmonic generation to identify the membrane disruption in Chinese Hamster ovarian cells under the exposure of light of 1869 nm (0.6 to 5.1 mJ and 0.5 to 4.0 ms). Their results indicated that there is very little membrane disruption in response to IR stimulation in this cell type,³⁶ whereas, Plaksin et al.¹⁹ and Farah et al.³⁷ observed that membrane effective capacitance and depolarizing displacement current are proportional to temperature's time derivative, dT/dt , as we can conclude this point from Eqs. (13)–(16). Here, the presented hybrid model shows the effects of dT/dt on changes of membrane capacitance and generation of action potential as seen in Figs. 5 and 6.

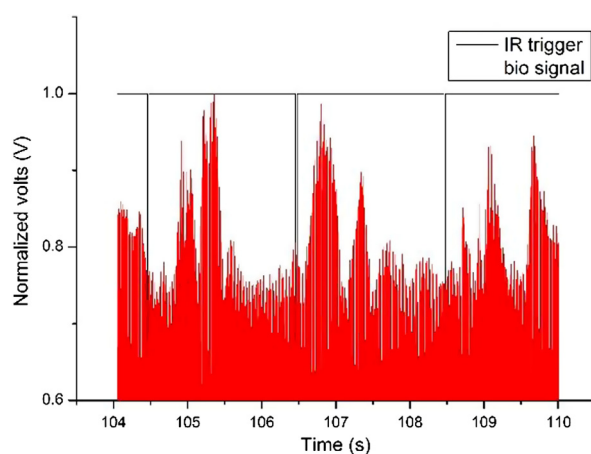


Fig. 6 Variation of measured voltage after laser pulse. The black line indicates the location of onset laser irradiation (the repetition rate of laser is 2 Hz).

4 Conclusion

The exact mechanism of INS is unknown, whereas the temperature rise is a crucial parameter in this process. Recent studies confirm this point that the membrane capacitance and displacement current are modulated by temperature rises during INS. Therefore, this study was aimed to investigate the effect of photo-heating on the initiation of an action potential. We utilized MHHM to explore how an action potential can initiate and propagate inside a typical axonal. Using this simulation, we estimated the threshold temperature rise to generate an action potential. Based on the simulated results and measuring the temperature rise of an aqua phantom, we could estimate the appropriate laser light parameter such as laser energy per pulse, repetition rate, and pulse width. Finally, we applied these results to optically *in-vivo* modulate neuronal activities of the earthworm. It seems that these findings can be applied to present a better understanding of INS opening new ways to neuronal modulation in the human studies.

Acknowledgments

VVT was supported by the Government of the Russian Federation Grant No. 075-15-2019-1885. The authors have no relevant financial interests in this article and no potential conflicts of interest to disclose.

References

1. R. Nardone et al., "Neurostimulation in Alzheimer's disease: from basic research to clinical applications," *Neurol. Sci.* **36**(5), 689–700 (2015).
2. M. W. Jenkins et al., "Optical pacing of the embryonic heart," *Nat. Photonics* **4**(9), 623–626 (2010).
3. Q. Xia and T. Nyberg, "Inhibition of cortical neural networks using infrared laser," *J. Biophotonics* **12**, e201800403 (2018).
4. G. H. Lee et al., "Multifunctional materials for implantable and wearable photonic health-care devices," *Nat. Rev. Mater.* **5**, 149–165 (2020).
5. J. M. Cayce et al., "Infrared neural stimulation of primary visual cortex in non-human primates," *Neuroimage* **84**, 181–190 (2014).
6. C. P. Richter et al., "Photons and neurons," *Hear. Res.* **311**, 72–88 (2014).
7. J. D. Wells et al., "Application of infrared light for *in vivo* neural stimulation," *J. Biomed. Opt.* **10**(6), 064003 (2005).
8. Y. T. Wang et al., "Infrared inhibition of embryonic hearts," *J. Biomed. Opt.* **21**(6), 060505 (2016).

9. M. J. Alemzadeh-Ansari et al., "Influence of radiant exposure and repetition rate in infrared neural stimulation with near-infrared lasers," *Lasers Med. Sci.* **34**(8), 1555–1566 (2019).
10. M. A. Ansari and M. Zakeri, "Blind localization of heating in neural tissues induced by a train of the infrared pulse laser," *J. Laser Med. Sci.* **10**(4), 264–267 (2019).
11. M. A. Ansari and R. Massudi, "Boundary integral method for simulating laser short-pulse penetration into biological tissues," *J. Biomed. Opt.* **15**(6), 065009 (2010).
12. R. Liljemalm et al., "Heating during infrared neural stimulation," *Lasers Surg. Med.* **45**(7), 469–481 (2013).
13. Y. Weissler et al., "Simulation of morphologically structured photo-thermal neural stimulation," *J. Neural Eng.* **14**(5), 055001 (2017).
14. M. Wang et al., "Prolonged post-stimulation response induced by 980-nm infrared neural stimulation in the rat primary motor cortex," *Lasers Med. Sci.* **35**, 365–372 (2020).
15. M. G. Shapiro et al., "Infrared light excites cells by changing their electrical capacitance," *Nat. Commun.* **3**, 736 (2012).
16. J. M. Cayce et al., "Calcium imaging of infrared-stimulated activity in rodent brain," *Cell Calcium* **55**(4), 183–190 (2014).
17. K. Eom et al., "Photothermal activation of astrocyte cells using localized surface plasmon resonance of gold nanorods," *J. Biophotonics* **10**(4), 486–493 (2017).
18. R. Liljemalm and T. Nyberg, "Quantification of a thermal damage threshold for astrocytes using infrared laser generated heat gradients," *Ann. Biomed. Eng.* **42**(4), 822–832 (2014).
19. M. Plaksin et al., "Thermal transients excite neurons through universal intramembrane mechano-electrical effects," *Phys. Rev. X* **8**(1), 011043 (2018).
20. A. G. Xu et al., "Focal infrared neural stimulation with high-field functional MRI: a rapid way to map mesoscale brain connectomes," *Sci. Adv.* **5**(4), eaau7046 (2019).
21. Z. Ebtehaj et al., "Computational modeling and validation of thermally induced electrical capacitance changes for lipid bilayer membranes irradiated by pulsed lasers," *J. Phys. Chem. B* **122**(29), 7319–7331 (2018).
22. F. Sohrabi, "One dimensional photonic crystal as an efficient tool for *in-vivo* optical sensing of neural activity," *Opt. Mater.* **96**, 109275 (2019).
23. https://www.sciencelearn.org.nz/image_maps/24-inside-of-an-earthworm.
24. A. V. Luikov, *Analytical Heat Diffusion Theory*, Academic Press (2012).
25. G. Arfken, *Mathematical Methods for Physics*, 3rd ed., Academic Press, Florida (1985).
26. Q. Liu et al., "Exciting cell membranes with a blustering heat shock," *Biophys. J.* **106**(8), 1570–1577 (2014).
27. M. Neimz, *Laser-Tissue Interaction: Fundamentals and Applications*, Springer-Verlag, Berlin (2002).
28. D. A. McCormick et al., "Neurophysiology: Hodgkin and Huxley model—still standing?" *Nature* **445**, E1–E2 (2007).
29. S. Fribance et al., "Axonal model for temperature stimulation," *J. Comput. Neurosci.* **41**(2), 185–192 (2016).
30. P. Schlett et al., "Towards safe infrared nerve stimulation: a systematic experimental approach," in *Proc. IEEE Eng. Med. Biol. Soc.*, pp. 5909–5912 (2019).
31. G. Throckmorth et al., "Comparing the efficacy and safety of infrared neural stimulation at 1450 nm and 1875 nm (conference presentation)," *Proc. SPIE* **10866**, 108660G (2019).
32. R. Deka et al., "Parameter extraction for neuron model simulation of action potential in earthworm giant nerve fiber," in *IEEE Int. Conf. Comput. Intell. and Commun. Technol.*, pp. 732–736 (2015).
33. X. Zhu, "Infrared inhibition and waveform modulation of action potentials in the crayfish motor axon," *Biomed. Opt. Express* **10**(12), 6580–6594 (2019).
34. E. H. Lothet et al., "Selective inhibition of small-diameter axons using infrared light," *Sci. Rep.* **7**(1), 3275 (2017).
35. H. T. Beier et al., "Plasma membrane nanoporation as a possible mechanism behind infrared excitation of cells," *J. Neural Eng.* **11**(6), 066006 (2014).

36. E. K. Moen et al., "The role of membrane dynamics in electrical and infrared neural stimulation," *Proc. SPIE* **9719**, 97190E (2019).
37. N. Farah et al., "Holographically patterned activation using photo-absorber induced neural thermal stimulation," *J. Neural Eng.* **10**, 056004 (2013).

Mohammad Ali Ansari is an assistant professor at Shahid Beheshti University. He is the head of Optical Bio Imaging Lab (OBIL). He received his MS degree and PhD in photonics from Shahid Beheshti University in 2005 and 2010, respectively. He is the author of more than 30 journal papers. His current research interests include optical imaging, near-infrared spectroscopy, and photoacoustic imaging.

Valery V. Tuchin is a corresponding member of the RAS, professor and chair of Optics and Biophotonics at Saratov State University. He is also the head of several laboratories in Russia. His research interests include tissue optics, laser medicine, tissue optical clearing, and nanobiophotonics. Tuchin is a fellow of SPIE and OSA, honored science worker of the Russia, honored professor of Saratov State University. He was awarded by SPIE Educator Award, FiDiPro (Finland), Chime Bell Prize of Hubei Province (China), Joseph W. Goodman Book Writing Award (OSA/SPIE), and OSA Michael S. Feld Biophotonics Award for pioneering research in biophotonics.